Biotemplated Nanostructured Materials†

Sofia Sotiropoulou,*,‡,§ Yajaira Sierra-Sastre,*,§,⊥ Sonny S. Mark,# and Carl A. Batt‡

Departments of Food Science and Chemistry and Chemical Biology, Cornell University, Ithaca New York 14853, and Department of Pathology & Laboratory Medicine, University of Pennsylvania Medical Center, Philadelphia, Pennsylvania 19104-4283

Received August 1, 2007. Revised Manuscript Received October 25, 2007

Biological materials naturally display an astonishing variety of sophisticated nanostructures that are difficult to obtain even with the most technologically advanced synthetic methodologies. As the needs for nanoengineered materials with improved performance characteristics are becoming increasingly important, the potential of biological scaffolds for the fabrication of novel types of nanostructures is being actively explored. This review presents an overview of "biotemplating" as an emerging, unique approach for the synthesis and organization of inorganic nanostructures into well-defined architectures. The technological significance of these architectures is emphasized. We review examples of biological templates explored to date (in terms of their origin and structure) and the success of a variety of methodologies in providing control over the size, crystallinity, and surface chemistry of the nanomaterials.

1. Introduction

Fast electronic systems, extremely sensitive sensor devices to probe confined environments and multiplexed techniques for high-throughput analysis, represent some of today's most prominent nanotechnological needs. The ultimate realization of these technological advancements will be based on our ability to synthesize and organize matter into controlled geometries on the nanoscale. During the past few years, the exploration of synthetic techniques for the fabrication of nanostructured materials having controllable morphologies has emerged as a fast-growing subfield of nanotechnology research. Advanced functional materials incorporating well-defined nanoarchitectures have shown great potential for nanotechnological applications, such as miniaturized nanoelectronics,[1] ultrafast quantum computing,[2] high-density memory/data storage media,[3] ultrasensitive chemical sensing/biosensing,[4] generation of high-efficiency catalytic substrates,[5] and high-throughput templating for the growth/attachment of other types of bio- or inorganic nanomaterials.[6,7] Of particular interest are one- and two-dimensional arrays of patterned nanostructures (nanoparticles, nanowires, nanotubes, etc.), which have been shown to display unique optoelectronic, magnetic, or catalytic properties that can be tuned by varying their size and/or interparticle separation distance. For example, patterned gold nanoparticles display plasmon optical properties that can be applied in surface-enhanced Raman scattering detection systems with high sensitivities,[8] whereas nanowires with high surface ratios and diameters in the 10–200 nm range display interesting optical and electrical properties that are highly desirable in electrochemical sensing technologies,[9] field-emission systems,[10] and lasers.[11] Nanoporous materials displaying molecular sieve properties can act as chemical sensor elements, wherein the plasmon properties of the pores can be used in optical detection systems (Raman, optical waveguides). One of the most important technological challenges that remain to be addressed, however, is the development of effective patterning methods to control materials assembly on a nanometer scale. At present, there is a wide variety of top-down and bottom-up fabrication techniques that are capable of creating nanostructured arrays with varying degrees of speed, cost, and structural quality. We shall provide a brief overview of some of these techniques below, but for more detailed descriptions, the reader is referred to several excellent recent reviews[12–15] and books.[16]

1.1. Top-down. Top down strategies involve either (1) using macroscopic tools to first transfer a computer-generated pattern onto a larger piece of bulk material, and then "sculpting" a nanostructure by physically removing material (e.g., through wet/dry etching); or (2) using macroscopic tools to directly add/rearrange ("write") materials on a substrate. In the first category, the most common techniques are based on photolithography, which is cost-effective and relatively fast, but its resolution is ultimately limited by optical diffraction effects to typically 0.2–0.5 μm. Electron- and ion-based lithographic methods, on the other hand, permit the creation of ordered nanostructured arrays with high resolution (i.e., $\leq$ 50 nm features and/or spacing) and allow very good control over particle shape and spacing; however, their throughput is limited; line-by-line pattern generation (a serial technique) is considered very slow when compared with a parallel technique (such as photolithography) in which the entire surface is simultaneously patterned all at once.

The second category of top-down approaches includes scanning probe lithographic (SPL) techniques (e.g., dip-pen

† Part of the "Templated Materials Special Issue".

* To whom correspondence should be addressed. E-mail: ss549@cornell.edu (S.S.); ys253@cornell.edu (Y.S.S.). Phone: 607-255-7902. Fax: 607-255-8741.
‡ Department of Food Science, Cornell University.
§ These authors contributed equally to this work.
⊥ Department of Chemistry and Chemical Biology, Cornell University.
University of Pennsylvania Medical Center.

10.1021/cm702152a CCC: $40.75
Published on Web 01/17/2008

nanolithography (DPN) and scanning tunneling microscopy (STM)), microcontact printing (μCP), and nanoimprint lithography (NIL). Currently, patterns generated using DPN can be as small as 15 nm, whereas STM offers the unparalleled capability to position individual atoms to pattern structures with ultrahigh, subnanometer precision. However, DPN and STM are also serial techniques and are therefore not suitable for high-volume manufacturing technologies, although this is a drawback that may eventually be overcome by the introduction of massively parallel microfabricated probe tip arrays.[17]

In contrast to the complex, technical demands of SPL-based methods, procedures for the parallel fabrication of nanostructures using μCP and NIL are remarkably simple and straightforward. A unique advantage of μCP is that the mechanical flexibility of the rubbery stamp allows conformal contact between the stamp and the substrate for a range of topologies, including curved substrates/inner surfaces inaccessible by conventional optical lithography schemes. One potential factor that can limit the resolution of μCP in some cases, however, is the availability of appropriate tools to generate features of appropriate sizes in the master hard mold used to produce the elastomeric stamp. In the case of NIL, the imprinting device can be reused numerous times, thereby providing for cost-effective, sub-100 nm lithographic replication. However, the initial fabrication of ultrahigh resolution master molds remains a difficult task in NIL and often requires the use of expensive EBL methods. Moreover, the whole process duration for imprinting and multilayer in-plane alignment is still considered too lengthy for large-scale, mass production applications.

In summary, top-down approaches offer a wide range of structures of high quality/yield, but are generally neither cost- nor time-effective, and for some methods, resolution below the 100 nm range is not easily achievable.

1.2. Bottom-up. The bottom-up approach takes advantage of physicochemical interactions for the hierarchical synthesis of ordered nanoscale structures through the self-assembly of basic building blocks. Currently, the most common types of bottom-up fabrication procedures are those based on the use of a templating substrate, such as chemically or topologically patterned surfaces, inorganic mesoporous structures, and organic supramolecular complexes (mainly block copolymer (BCP) systems[18]). Topographically/chemically patterned surfaces have shown to be particularly effective in directing the nucleation and growth of 1D/2D colloidal crystals or highly uniform colloidal aggregates with well-controlled sizes, shapes, and structures. But even so, the fabrication of the substrate template requires a separate pre-step using traditional top-down fabrication techniques. BCPs provide another versatile route for templating the self-assembly of ordered nanoscale structures (metallic nanoparticles and other inorganic materials), particularly on surfaces. The periodicity of the microphase-separated domains in BCP systems is typically in the range of 10–200 nm. However, the main disadvantage to the use of block copolymer templates is the requirement in some cases of the synthesis of highly specialized polymeric components that may not be readily or commercially available. In addition, the precise control over the formation of stable microdomains with the desired spatial location/orientational order as well as the elimination of various defects remain as great challenges for most BCP-based templating schemes and typically require the introduction of external fields (e.g., mechanical flow fields and/or electromagnetic biases, etc.).[19]

An alternative parallel approach that is emerging for the bottom-up synthesis of nanostructured materials is the use of biological-based templates ("biotemplating"). Stimulated by nature's fascinating examples, researchers aiming to construct nanometer-scale devices and systems have begun to explore novel bottom-up synthesis routes lying at the interface of the inorganic and biological worlds. Such investigative efforts fall under the realm of "nanobiotechnology," a recently coined term describing the field of interdisciplinary research emerging from the convergence of nanotechnology, engineering, and molecular biotechnology.[20] The term, initially a quite narrow one referring specifically to the employment of technological advances to probe fundamental biological questions, has now broadened in scope to include other fields of research aimed at harnessing naturally occurring processes and structures for the fabrication of technologically relevant structures. Indeed, this branch of nanobiotechnology (sometimes also referred to as "bionanotechnology") is an interdisciplinary field that has grown sufficiently in the past decade into what can now be distinguished as two major areas of investigation: (1) biomimicry, the design of synthetic organic/inorganic materials based on principles found in nature, and (2) biotemplating (or "bionanofabrication"), a process that takes advantage of the structural specificity or catalytic activity of biological systems to create novel types of micro/nanostructured materials. Biotemplating is showing great promise in organizing nanomaterials into well-defined architectures. Recent advances in the field of biotemplating, along with the technological significance and some potential applications of biotemplated materials, are the main focus of this review.

2. Aims, Scopes, and Limitations of the Review

Within the last 5 years, there has been incredible progress in the field of biotemplating. Researchers have managed to achieve astonishing levels of control over the biological−inorganic interface leading to highly uniform nanostructures. Such efforts are helping to address some of the major challenges in the development of advanced nanotechnological devices and serve to demonstrate how biotemplating is emerging as an effective new route for the nanofabrication of novel materials. Recent reviews on bionanofabrication[21] and biomimetism[22] have contributed significantly to establish definitions and have provided information on certain selected aspects of the field of nanobiotechnology. This new review specifically aims to provide the reader with an overview of biotemplating as an approach to organize nanomaterials into one- (1D), two- (2D) or three-dimensional (3D) technological platforms. Nanoparticles (NPs), nanowires (NWs), and nanotubes represent technologically interesting nanostructures that all have potential applications as components in advanced optoelectronic devices, catalytic systems, etc., and are the focus of

this review. Another class of nanostructures that has been included in this review involves nanoporous materials fabricated from complex biological templates. Such materials are potentially interesting for sensing applications (photonic devices, biosensors) or as 3D architectures that can be further used for the synthesis of higher-ordered structures.

This review is organized into three main categories on the basis of the origin of the biological template employed: (1) (micro)organisms (i.e., organisms, diatoms, viruses, bacteria), (2) design-based biomacromolecular building blocks (i.e., natural or synthetic lipids, peptides, DNA oligonucleotides), and (3) proteins. For each section, the technologically relevant properties of the biological material are discussed, followed by a description of the fabrication approaches used, and the achieved quality of the final nanostructures (with respect to dimensions, uniformity and orientation). The use of the biotemplated nanostructures in device fabrication and the corresponding performance characteristics are also described whenever such examples are available in the literature. Figure 1 illustrates the various classes of biological templates discussed, with some representative examples, placed alongside the length scale according to their critical dimensions.

3. Biotemplating Mechanisms

Biotemplating seeks to either replicate the morphological characteristics and the functionality of a biological species or use a biological structure to guide the assembly of inorganic materials. In the first case, the biological substrate has interesting morphological characteristics (e.g., diatoms, butterfly wing scales, viruses) and metal replication is used to provide a more stable and more controllable synthetic substrate. The replication process typically leads to the generation of either a negative, positive (or hollow), or exact copy of the template. Indeed, a large variety of biological species have been used as templates: bacteria, textiles/paper, hair, cells, insect wings, spider silk, wool, and wood; see ref 34 and references therein. The majority of the biological structures that have been used for replication show nanoporous features (e.g., diatoms), channels (viruses), and other complex hierarchical architectures (butterfly wings). The level of precision in replicating nanoscale topographies and features is the major challenge. In the second case concerning the biologically guided assembly of nanomaterials, a natural biological system is used to nucleate inorganic structures and promote pattern formation. This is ubiquitously directed by covalent/noncovalent interactions and molecular recognition processes. For such interactions to take place, the biological structures must present specific physicochemical and/or morphological attributes to direct the assembly of inorganic structures into technologically useful platforms.[35] Such attributes can include a secluded inner channel or inner cavity that is accessible only by molecules of specific size/charge, or the presence of a unique functional group at specific locations.

4. Biotemplating using (Micro)Organisms and Viruses

In nature, there are a large number of biological systems that display morphologically complex architectures potentially suitable for templating. Indeed there is already quite a long list of biological materials that have been successfully replicated for the formation of artificial structures, and these include (but are not limited to) cotton/cloth, pine wood, human and animal hair, silk, and wool. However, among the various replicated structures reported, only a few have shown technological interest so far and these are discussed further below.

4.1. Butterfly Wings. Butterfly wings exhibit a variety of beautiful colors that are not only the result of pigments but more importantly are due to the presence of periodical submicrometer structures (scales, Figure 1). Butterfly wing scales ($\sim$150 μm long and $\sim$50 μm wide are typical dimensions) show an extremely complex morphology consisting of aligned lamellas, which are in turn arranged into highly ordered architectures forming pores and layers. This complex structure has been used to biotemplate tubular ZnO structures of micrometer dimensions.[36] Interestingly, it has been found that the precise replication of the structural hierarchy of this biological structure using atomic layer deposition of Al_2O_3 coatings also replicates the optical properties,[23] providing a direct way to obtain photonic devices with functions similar to optical waveguides and beam splitters. Potyrailo et al.,[37] for example, found that these nanostructured architectures show properties of photonic structures, and upon interaction with different chemical vapors produce diverse differential reflectance spectra, achieving highly selective responses using a single structure. Compared to artificial photonic sensors, the butterfly wing scale optical structures showed higher selectivity, obtaining a large difference in reflectance spectra in the vapors of solvents with similar polarities and refractive indices (water, ethanol, methanol) without compromising their sensitivity, which remained in the same range as the artificial systems (i.e., 1–2 ppm). This is of great importance, because selectivity has often been a major hurdle in the synthesis of artificial sensors; typically, this is an issue that can only be addressed by applying chemically selective coatings that introduce additional steps in the fabrication, are not stable, and are not standard for all analytes.

4.2. Diatoms. Diatoms are unicellular photosynthetic microorganisms with sizes in the 1–100 μm range. More than 10 000 species of diatoms are known, and they are characterized on the basis of the shape and structure of their cell walls, which naturally incorporate ("biomineralize") silica. These silica cell walls have unique nanostructured patterns in the range of 50 nm that can be hexagonal, rod-shaped, or circular depending on the species (Figure 2). The biological (in vivo) mechanism of silica precipitation and pattern formation has been elucidated and such studies reveal that there is a striking level of control over the size of the precipitated silica, with size distributions that are close to being monodisperse.[38]

Mirkin and co-workers were the first to show that diatom silica walls could be chemically programmed to interact with inorganic nanoparticles.[39] In those studies, a piranha etch solution (sulfuric acid/hydrogen peroxide mixture) was used to digest the organic components of the diatoms and activate the cells walls for subsequent aminosilane functionalization. The amino-functionalized diatoms were then reacted with

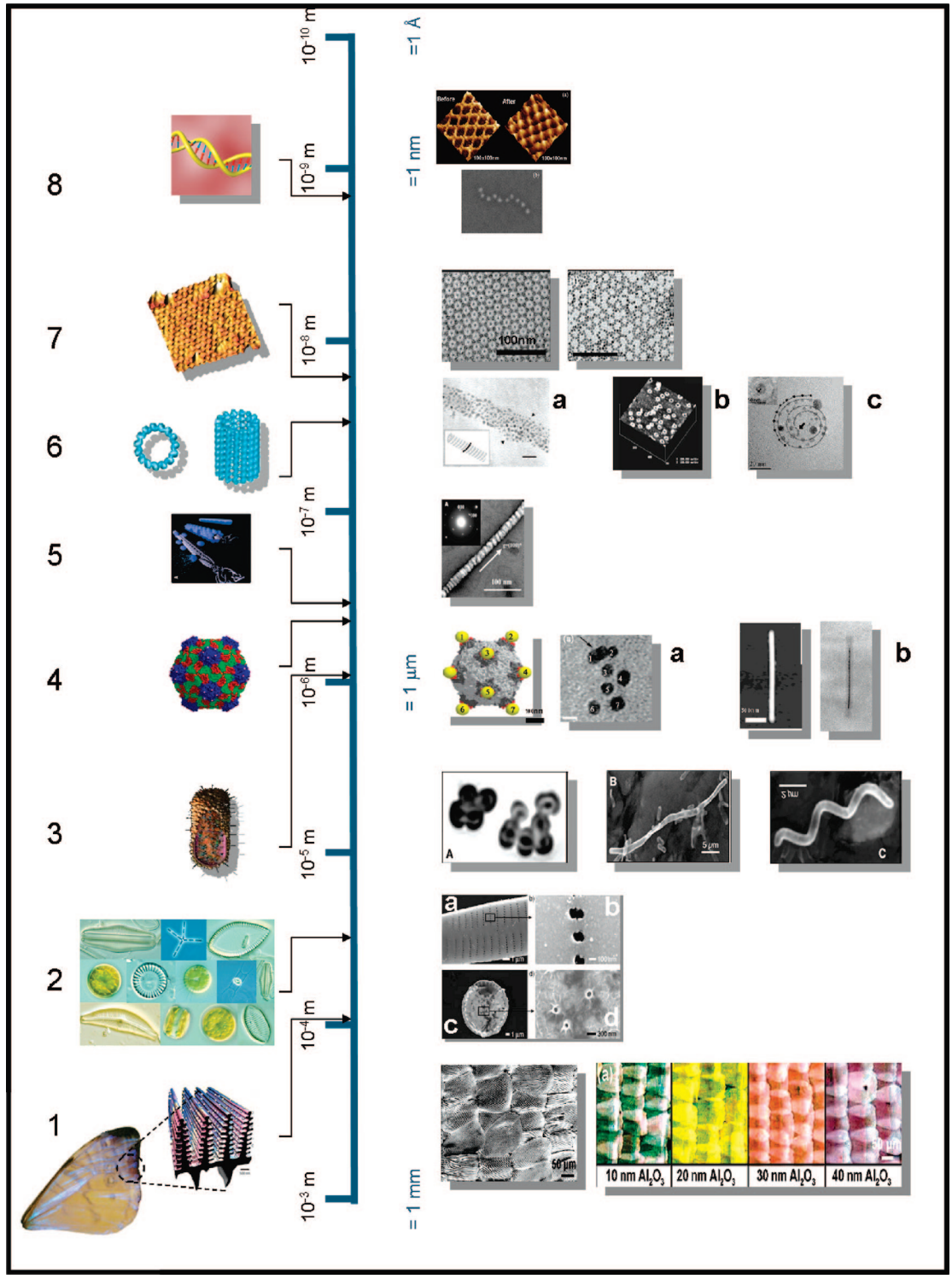

Figure 1. Overview of biological templates, placed alongside the length scale according to their critical dimensions. On the left-hand side, schematic representations of the biological structures are shown, whereas the corresponding templated structures synthesized are displayed on the right-hand side. (1) Butterfly wing scales. SEM image of the alumina template and optical images of their tunable photonic properties.[23] (2) Diatoms. SEM-images of (a, b) Synedra and (c, d) Thalassiosira frustules coated with silver (30 nm).[24] (3) Bacteria. Microscope (optical and electron) images of metallized microspheres from *D. radiodurans*, microfilaments from *E. coli*, and microcoils from *R. rubrum*. [25] (4) Mosaic virus (model of the cowpea mosaic virus).[26] (a) Gold nanoparticles bound to CPMV virus. An arrow marks a 5-fold axis with two particles bound (TEM image and model).[26] (b) AFM image of the tobacco mosaic virus and TEM image of a 3 nm diameter Ni nanowire cast within the inner channel.[27] (5) M13 bacteriophage virus. Dark-field diffraction contrast image of a ZnS viral nanowire with specific crystallographic ordering.[28] (6) Microtubules. (a) TEM image of Pd NPs on a microtubule.[29] (b) SFM image of tubulin structures. (c) TEM image of Ag nanoparticles on tubulin spirals.[30] (7) S-layer proteins (from *D. radiodurans*). TEM image of the native and quantum dot-functionalized S-layer from *D.radiodurans*.[31,32] (8) DNA. AFM image of a 4 × 4 self-assembled DNA "grid" functionalized with Au nanoclusters (SEM).[33] Figure 1.1 reprinted with permission from ref 23. Copyright 2006 American Chemical Society. Figure 1.2 reprinted with permission from ref 24. Copyright 2005 Wiley. Figure 1.3 reprinted with permission from ref 25. Copyright 2005 Elsevier. Figure 1.4 reprinted with permission from ref 26. Copyright 2004 American Chemical Society. Figure 1.5 reprinted with permission from ref 28. Copyright 2004 American Association for the Advancement of Science. Figure 1.6 reprinted with permission from refs 29 and 30. Copyright 2002 and 2006 Wiley. Figure 1.7 reprinted with permission from refs 31 and 32. Copyright 2004 and 2006 American Chemical Society.

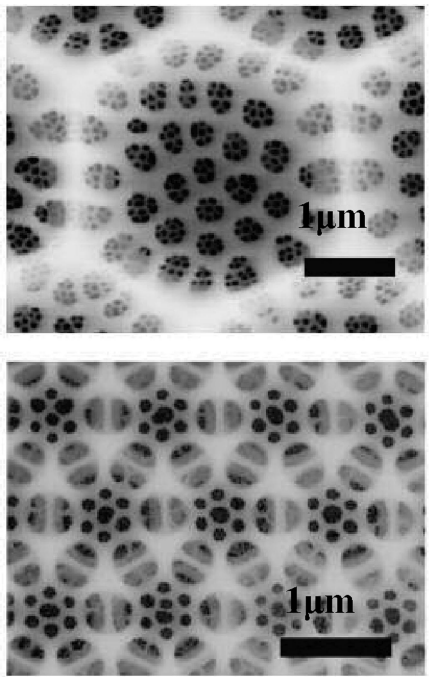

Figure 2. Scanning electron microscopy (SEM) images of cell wall structures from the diatoms (upper panel) *Coscinodiscus asteromphalus* (lower panel) and *Coscinodiscus granii*. Reprinted with permission from ref 38. Copyright 2006 Wiley.

ssDNA and used as templates for the directed organization of Au nanoparticles functionalized with the cDNA. The nanoparticles formed a near-monolayer following the surface morphology and shape of the diatom template. The same group was also successful in fabricating metal replicas that were identical to their respective diatom templates in nanostructure surface features, preserving even sub-200 nm pore structures and other sub-100 nm topological features (Figure 1, panel 2).[24] Diatom frustules have also been used as masks for the evaporation of Au films, resulting in the fabrication of membranes with complex 3D morphology that represent the exact negative of the porous frustule used as template.[40]

The ability to exactly replicate the diatom silica shell holds great promise for technological applications. Indeed, metal-coated diatom frustules and diatom-templated metallic shells were recently examined as potential surface-enhanced Raman spectroscopy (SERS) surfaces.[24] Both types of structures displayed SERS signals upon exposure to rhodamine 6G (R6G), which in the first case allowed detection of 1 mM R6G and in the second case was greatly enhanced, allowing detection down to 100 nM. Other optical properties attributed to the nanotopographic features of the silica shell, such as their photoluminescence properties, which are sensitive to organic vapors and gases,[41] still remain to be fully explored.

4.3. Bacteria. Bacterial microorganisms offer a range of advantages for the templating of nanostructures. Ease of preparation, potential for genetic manipulation, and commercial availability are the most attractive characteristics. Furthermore, bacteria have evolved a large variety of well-defined morphologies that are precisely controlled in vivo at the micro- and nanolevel. Cocci-, bacilli-, and spirilli-shaped bacteria can lead to the formation of corresponding 3D hollow nanostructures that are currently unattainable with other techniques. For example, cells from certain species of bacteria have served as sacrificial templates for the formation of ZnS hollow spheres (*Lactobacillus streptococcus thermophilus*) and hollow nanotubes (*Lactobacillus bulgaricus*) that maintain the size and morphology of the initial bacterium.[42] Silica particles[43] have also been templated on bacterial threads, resulting in the formation of silica fibers formed by densely compacted nanoparticles. Calcination of these bacteria−silicate structures, removed the organic matrix and resulted in an organized array of 0.5 μm wide channels.

Deinococcus radiodurans, *Escherichia coli* and *Rhodosprilium rubrum* were all used in the same study to template magnetic (nickel) nanoparticles (Figure 1, panel 3).[25] The cells were initially activated with catalytic Pt, and Ni nanoparticles were then deposited via an electroless deposition process from a $NiSO_4$ solution. The resulting structures included nanospheres, nanofilaments (45–80 nm long), and nanocoils (9 μm long).

In an attempt to achieve the specific functionalization of bacterial cell wall components, some studies have been carried out using live bacteria in order to take advantage of their high affinity to specific factors (such as lysine). For example, *Bacillus cereus* bacteria that have high affinity for lysine were covered with lysine-functionalized Au nanoparticles, (30 nm diameter), producing an electrically conductive monolayer.[44] The selectivity and high density of nanoparticle patterning allowed the formation of a percolating monolayer characterized by a dramatic increase in conductivity and serving as an on/off switch. The same concept can be applied not only to electrical systems but also to electro-optical ones if used in conjunction with electroluminescent nanoparticles or quantum dots, demonstrating the versatility of the approach.

4.4. Viruses. *4.4.1. Mosaic Virus Family.* Members belonging to the family of mosaic viruses (including tobacco, red clover, cowpea, brome, and cowpea chlorotic mottle virus (CCMV)[45]) are regarded as an attractive class of biotemplates because of their high stability in extreme pH conditions and temperatures (as high as 60 °C in some cases). Furthermore, their viral capsids consist of repeating patterns of charged amino acids that are amenable to chemical functionalization approaches.

Tobacco mosaic virus (TMV) comprise linear-shaped particles that are 300 nm long and 18 nm wide and contain an internal channel that is 4 nm in diameter. In 1999, Shenton et al. were the first to demonstrate that TMV particles could be used for the deposition of a variety of nanoparticle types, including CdS (5nm diameter), PbS (30 nm diameter), and FeO (22 nm diameter). In this case, the nucleation and growth of the nanoparticles is guided by the charged residues located on the outer surface of the virus. Mineralization was also possible using sol–gel chemistry, which resulted in a thin silica coating on the virion surface. In fact, the silica-coated virions showed an even higher level of ordered structure by self-assembling into linear chains.[46] In this initial paper, it was shown that functionalization produced hollow structures, but later genetic engineering of the virus allowed for selective deposition to take place either at predefined positions on the outer surface or even inside the hollow channel.[47] The

selective deposition of nanoparticles inside the hollow channel of the virus also led to the formation of Ni and Co nanowires[27] several micrometers long and only a few nanometers (~3 nm) in diameter (Figure 1, panel 4b).

TMV particles have also been used to produce porous silica structures. Fowler et al.,[48] for example, reported the possibility to use the virus particles to produce mesoporous and mesostructured silica. They took advantage of the natural tendency of the virus particles to form nematic liquid crystals at high concentrations, and then used these as a template to produce structured silica with a periodicity of 20 nm. It was determined that the coaligned TMV particles were intercalated within a continuous framework of silica. Successful replication in this case was dependent on matching the hydrolysis rate of the silicates and the time required for realignment of the TMV particles. The same TMV particles were also found to become radially aligned into 3D silica nanoparticles (100–150 nm diameter) if the amount of silica is decreased so that mineralization proceeds at a slower rate.

Three-dimensional patterns were also fabricated using a genetically engineered cowpea mosaic virus[26] (Figure 1, panel 4a). Here, cysteines were introduced to selectively bind gold nanoparticles to the virus exterior, producing well-defined 3D patterns. This approach allowed for exerting control over the interparticle distance by simply altering the location of the inserted cysteine residue. Finally, bimetallic alloys of CoPt and FePt nanowires have also been fabricated[49] preferentially within the inner channel of TMV, further expanding the range of applications of this template.

4.4.2. Other virus families. Apart from the mosaic viruses, the spherical *Chilo iridescent virus* (CIV)[50] as well as the filamentous *fd* virus[51] have also been used as biological templates. CIV consists of a layered structure that has a dsDNA–protein core surrounded by a lipid bilayer. This, in turn, is surrounded by an inner−outer capsid shell, where fibers greater than 35 nm in length protrude outward from the surface. Gold nanoparticles could be seeded around the viral capsid by carefully optimizing the ionic strength and pH of the solution (thus affecting the noncovalent interactions of the Au nanoparticles with the fibrils). In contrast, the *fd* virus (length 880 nm, diameter 6.6 nm) has been used to template some interesting silica structures. By hydrolyzing tetraethylorthosilicate (TEOS) under acidic conditions, silica nanorods (20 nm diameter), silica nanowires, and bow-tie-shaped silica bundles are formed because of electrostatic and/or hydrogen-bonding interactions between silica precursor molecules and the organic substrate.

Research in the area of virus-templated nanostructures has recently been revolutionized by the work of Belcher and co-workers at the Massachusetts Institute of Technology, who demonstrated the use of M13 bacteriophage as a universal template to control the patterning of semiconducting, metallic, oxide, and magnetic materials. In their work, the protein comprising the viral capsid was genetically modified with substrate-specific peptides generated through the use of phage-display techniques.[28] This allowed the formation of ZnS and CdS nanocrystals at site-specific locations within the viral capsid structure in a very controlled manner. Indeed, not only could the nucleation of nanocrystals be directed at

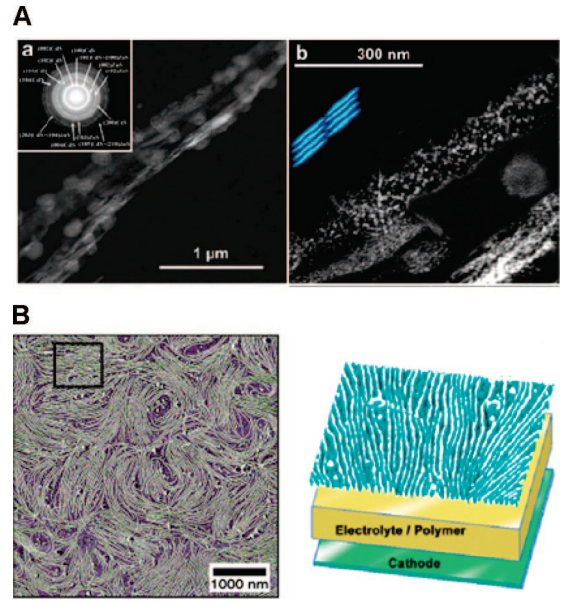

Figure 3. (A) ZnS−CdS hybrid nanowires prepared from genetically modified M13 bacteriophage. Reprinted with permission from ref 52. Copyright 2003 National Academy of Sciences. (B) Co_3O_4 nanowires in a two-dimensional assembly driven by liquid-crystalline ordering of engineered M13 bacteriophage viruses (phase-mode Atomic Force microscope image). Reprinted with permission from ref 56. Copyright 2006 American Association for the Advancement of Science.

specific sites corresponding to the location of the engineered peptides, it was further shown that mineralization was influenced by the peptide orientation, thus allowing the production of nanocrystals displaying preferred crystalline orientations (Figure 1, panel 5). Annealing of the nanocrystals after removal of the organic template led to the formation of single-crystalline nanowires of the same crystallographic orientation as the precursor nanocrystals. The fabrication of highly oriented quantum dot nanowires was also demonstrated, as well as the possibility to assemble hybrid nanomaterials (Figure 3).[52] In other work by the Belcher group, virus-templated gold nanoparticles were used for the subsequent nucleation and growth of cobalt oxide nanowires[53] into 2D architectures over large scales. Their results indicated a very good dispersion of the Au−Co hybrid material. Taking this work even further, the same group then used the principles of self-assembly to organize virus−virus interactions such that a 2D liquid crystalline layer was created on top of polyelectrolyte films. When these ensembles were then tested for lithium-battery applications, a potential for achieving high cycling rates was observed, with capacity remaining practically stable for up to 10 charge/discharge cycles. Moreover, the devices could be operated at equivalent or higher capacitance values when compared to conventional Li battery configurations currently reported in the literature.[54,55] According to the authors, the total power output of their systems can potentially be increased by simply assembling a larger number of alternating stacks of the material (Figure 3B).[56]

5. Biotemplating using Self-Assembled Architectures Derived from Biological Macromolecules

In nature, self-assembly is the major driving force to fabricate a vast array of supramolecular architectures. For

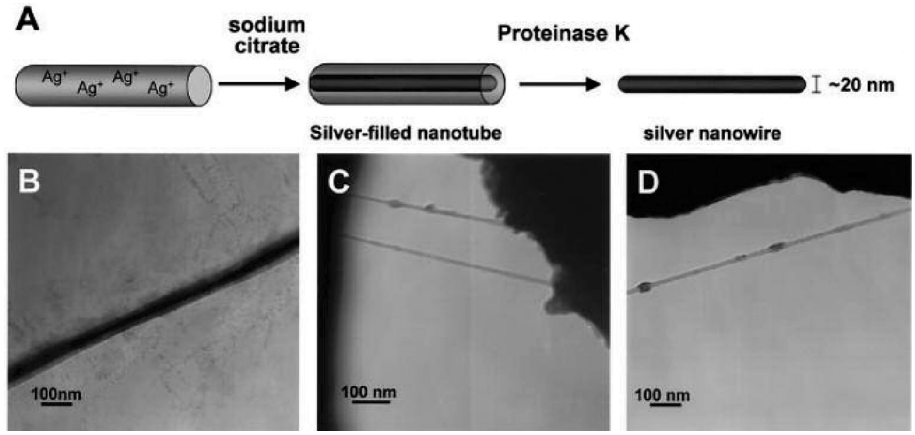

Figure 4. Casting of silver nanowires using peptide nanotubes. (A) The nanowires are formed by the reduction of silver ions within the tubes, followed by enzymatic degradation of the peptide mold. (B) TEM analysis (without staining) of peptide tubes filled with silver nanowires. (C, D) TEM images of silver nanowires that were obtained after proteolytic lysis of the peptide mold. Reprinted with permission from ref 60. Copyright 2003 American Association for the Advancement of Science.

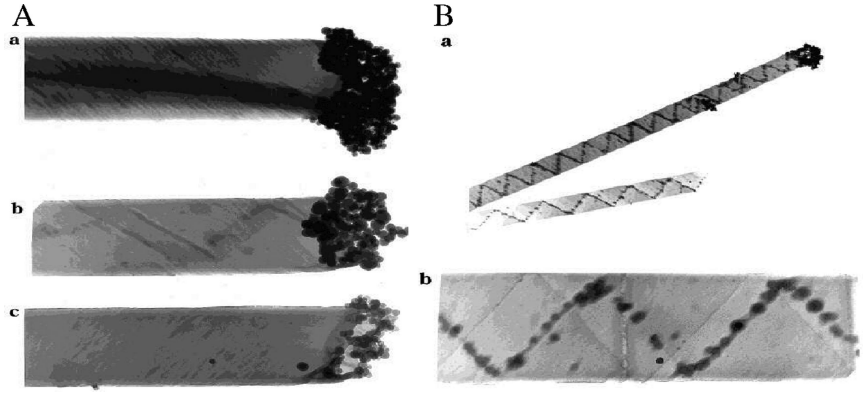

Figure 5. TEM images of lipid templating of Au NPs at (A) the caps of the tubes or (B) in helical structures. Reprinted with permission from ref 63. Copyright 2000 American Chemical Society.

example, lipid molecules form micellar droplets in water, whereas peptides and proteins assemble into functional structures that guide the formation of cellular components and even inorganic biomaterials such as bone. The same molecules that are used in nature can also be used for patterning nonbiological components. Therefore, self-assembled architectures derived from various types of biomacromolecules, including lipids, peptides/proteins and DNA, have all been used for biotemplating.[57]

5.1. Design-Based Biomacromolecular Building Blocks for Biotemplating. The structure of lipids, peptides, and DNA allows for their precise manipulation and further enables the synthesis of higher-order supramolecular structures, with tunable properties. The notion of "design-based" biological templates (first introduced by Payne[58]) refers to the use of biological templates wherein each of the building blocks have been specifically designed and self-assembled into predetermined conformations.

5.1.1. Peptides. Peptides, which are linear assemblies comprising 2–30 amino acid residues, can be designed to self-assemble into a large variety of structures.[59] For example, suitably designed peptides can be self-assembled into tubular structures (using aromatic peptides), ordered fibrillar structures (using charge-complementary peptides), or even nanospheres. Furthermore, a cyclic octapeptide with alternating L and D aminoacids can self-assemble into nanotubular structures that further assemble into crystalline arrays. Along similar lines, linear hepta- and octapeptides can self-assemble into tubular structures, as well. Hence, peptides have recently emerged as easily amenable building blocks for creating nanotubular structures via self-assembly processes. The inner hollow channel of these structures can in turn be used to cast metal nanowires, and, indeed, 20 nm Ag nanowires have been successfully fabricated using such an approach.[60] The proteolytic degradation of the template further allowed the isolation of discrete robust nanowires (Figure 4). Finally, Matsui and colleagues[61] have reported the successful use of histidine-functionalized peptide nanotubes to template the formation of metallic nanowires. In this case, gold nanocrystals (6 nm average diameter) were synthesized directly on the histidine-rich peptide templates by the in situ reduction of $ClAu^{3-}$ with $NaBH_4$.

5.1.2. Lipids. Lipids can be guided to self-assemble into a variety of structures by fine-tuning the composition of the lipid molecules and by carefully controlling the synthetic conditions. Certain types of structure, in particular lipid tubes (0.5 μm diameter and 20–100 μm length), have been employed as biotemplates for the fabrication of metallic cylinders using metallization (Figure 5).[62] Perhaps more importantly, charged lipid tubules can also serve as effective templates for the fabrication of 3D architectures and even novel helical structures. For this approach, alternating layers

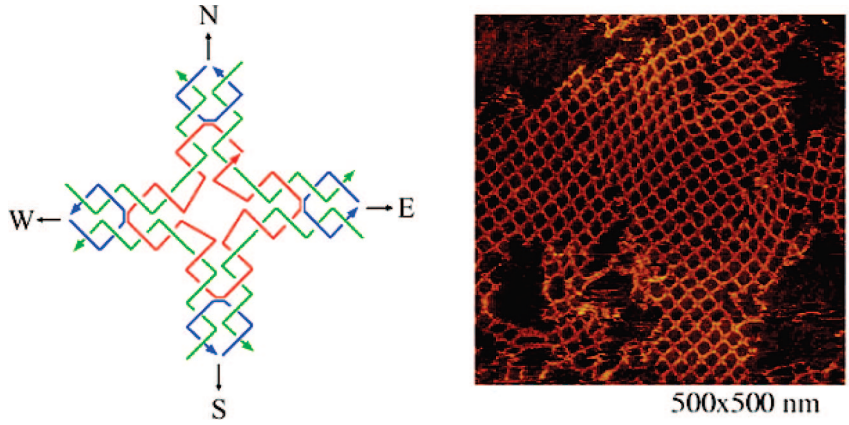

Figure 6. (A) Self-assembly of DNA nanogrids using a 4 × 4 DNA strand structure. (B) AFM image of the resulting 2D lattice (nanogrid). Reprinted with permission from ref 122. Copyright 2003 American Association for the Advancement of Science.

of anionic/cationic polymers were[63] used for the organized adsorption of silica particles as small as 45nm.

5.1.3. DNA. DNA is the basic information storage molecule in nature, comprising two complementary strands held together by hydrogen-bonded base pairs (adenine (A)−thymine (T) and guanine (G)−cytosine (C)). This complementary base-pairing mechanism drives the formation of the classical double-helix structure of DNA. The nanometer-scale width dimensions of the DNA molecule (diameter of 2 nm), along with its helical pitch of 3.4–3.6 nm, make it a very attractive template for nanotechnological applications.[64] Hence, DNA has been used extensively as a building block for biotemplating experiments; in fact, DNA is the single most common biological template investigated to date. The subject matter, therefore, is quite extensive and a full consideration is outside the scope of this review. We shall only briefly review here the most recent advances in the field of DNA-templated nanoparticle arrays; for a more comprehensive treatment of other types of DNA-templated nanostructures, the reader is referred to several recent reviews that have been published.[65–71]

Linear single-stranded DNA templates have been used to direct the ordered assembly of Au nanoparticles tagged with complementary oligonucleotides. Here, the placement of the nanoparticles along the DNA template is guided either by the molecular recognition properties of the two complementary strands or by electrostatic interactions with the negatively charged backbone of DNA.[72] One-dimensional metallic, semiconducting, and magnetic nanoparticle arrays have all been successfully reported[73] with good control over the dimensions, crystallinity, and even chirality.[74] Significantly, the mean distance between neighboring Au nanoparticles can be controlled by the length of the templating DNA molecules. Nanowires with diameters as small as 15 nm and displaying a variety of physicochemical properties (metallic,[75] fluorescent,[76] magnetic,[67] and even binary semiconductors[71]) have also been successfully fabricated.

It should be noted, however, that the simple hybridization of single-stranded oligonucleotides is generally not sufficient for the fabrication of more complex types of structures and architectures. Hence, synthetic DNA molecules featuring branched junction motifs have been designed. "Sticky ends" flanking the junctions enable the self-assembly of these novel DNA sequences into 2D and 3D architectures, such as lattices and grids (Figure 6).[77,122] These structures can, in turn, be further utilized for the templated assembly of nanoparticles (as small as 5 nm) into ordered periodic arrays with excellent control over the lattice spacings (interparticle distances ranging from 15 to 38 nm).[78] Synthetic DNA molecules have also been used as templates for the fabrication of ultrathin nanowires, featuring diameters down to 15 nm.[33] The ability to control the spatial organization of NPs using robust DNA motifs[79] has now led to the synthesis of binary arrays of nanoparticles displaying different sizes (i.e., 5 and 10 nm diameter NPs). More recently, Aldeye and Sleiman[80] reported the design of "dynamic" single-stranded and cyclic DNA templates that allow for geometrical modularity of the nanoparticle assemblies. Using their approach, the authors demonstrated exceptional control over not only the spatial positioning of each nanoparticle but also their geometrical assembly. Moreover, the authors' ability to perform write/erase functions further exemplified the unique possibilities afforded by DNA in materials templating applications.

5.2. Protein-Based Biotemplating. *5.2.1. Protein Fibers.* In biological systems, protein fibers comprise a large class of structural biomaterials that play an essential role in the motility, elasticity, scaffolding, stabilization, and protection of cells, tissues, and organisms.[81] Because of their unique morphological properties and molecular recognition capabilities, fibrous proteins have been employed as scaffolds for the templated assembly of semiconducting quantum dots (QDs)[82] and for the in situ deposition of various metallic species in a variety of interesting nanoarchitectures.

Tubulin is an important fibrous protein from eukaryotes that has been employed for the biotemplate-based nanofabrication of linear nanoparticles arrays,[29,83,84] nanowires,[83–86] spirals, and nanometer-sized ring structures.[30,87] Tubulins are the basic building blocks of microtubules (MTs), cylindrical structures within cells that govern the location of membrane bound organelles and serve as tracks for guiding cargo transportation. Importantly, MTs can be assembled in vitro from tubulin under appropriate conditions of temperature, pH, and ionic strength and in the presence of cofactors. Behrens et al. has demonstrated the use of these highly ordered linear tubulin assemblies for the template-directed deposition of Au,[30] Ag,[30,83] Pd,[29,84] and FePt[84] via electroless deposition techniques. Metallic nanoparticles (2–5 nm d.)

were synthesized in situ when the MTs were incubated with metal ion precursors, followed by the addition of reducing agents such as $NaBH_4$, dimethylamine borane, and hydroquinone. Molecular modeling studies confirmed that the formation of the metallic superlattice arrays was achieved because of nanoparticle binding to defined patterns of amino acid residues accessible for binding at the tubulin surface (Figure 1, panel 6a). In other words, the arrangement of the nanoparticles reflects the helical arrangement of the tubulin subunits within the MT template. The high aspect ratio of MTs, with typical dimensions of about 25 nm in diameter and several micrometers in length, makes them an attractive template for the fabrication of nanowires. Indeed, exposure to high metal concentrations leads to a quasi-continuous metal coating on the MTs.

In the presence of Ca^{2+} ions during the in vitro self-assembly of tubulin, other polymorphic structures with geometries different from that of MTs can be achieved. For example, ring-shaped and spiral tubulin assemblies have also been employed as metallization templates[84,87] (Figure 1, panels 6b and 6c). Measurements of the mean interparticle distance indicate the deposition of one Ag particle per tubulin dimer.

Other fibrillar proteins such as amyloid fibers are emerging as excellent candidate templates that can withstand diverse metallization procedures necessary for creating electronic circuits in industrial settings.[86] Amyloid fibers are formed in Alzheimer's-related disease states[88] and also in vitro by many proteins and peptides unrelated to any such disease. Genetically engineered amyloids containing surface-accessible cysteine residues were used to covalently link Au colloids.[85] These metallized fibers were placed across Au electrodes and additional metal was then deposited to gain conductivity. The biotemplated metal wires showed low resistance and ohmic behavior, properties found in conducting solid metal wires. (Figure 7).

In addition to genetically engineered amyloid fibers, bioengineered flagellin proteins are also being actively investigated as nanotube templates.[89] Flagella are elongated helical assemblies of flagellin proteins, up to 10–15 μm in length, that act as propellers of motion in bacterial cells. Kumara et al. have shown the display of rational designed peptide loops of genetically engineered flagella[82,89,90] that yielded ordered arrays of binding sites for metal ions, which can be used as precursors for the generation of nanotubes. From the six metal ions used in this study, 5.0 mM Cu(II) ions complexed with imidazole in the histidine loop peptides. After reduction with $NaBH_4$, Cu nanotubes were produced with diameters of approximately 100 nm. The ability to introduce peptide loops to flagellin monomers separated by 5 nm resulted in evenly spaced binding sites for the generation of ordered arrays of nanoparticles and uniform nanotubes. It is envisioned that removal of the flagellin protein template in a controlled manner will ultimately yield pure hollow Cu nanotubes. A recent report further demonstrates the use of flagella as scaffolds for the self-assembly of 3 nm ZnS/Mn and CdTe QDs.[82] Flagella without any inserted histidine loop peptides did not result in the self-assembly of QDs under the same conditions. These results confirm the feasibility of using genetically engineering approaches for the creation of fibrillar proteins that can control the subsequent deposition of nanomaterials in a regular fashion.

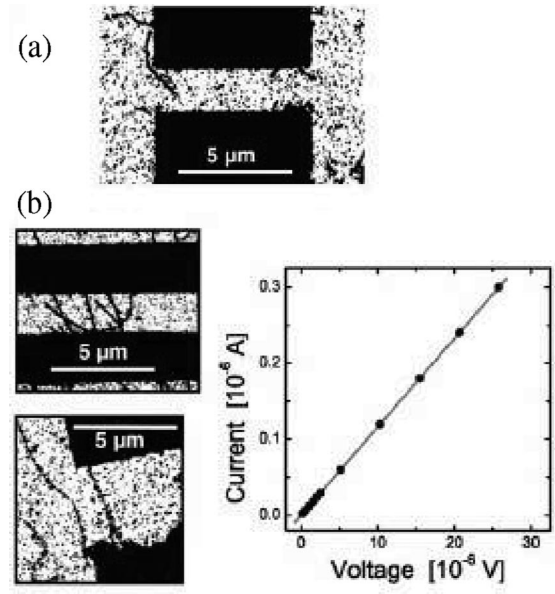

Figure 7. Gold amyloid fibers deposited on patterned electrodes. (a) Gold nanowires that did not bridge the gap between two electrodes did not conduct. (b) Gold nanowires bridging the gap between two electrodes (left) exhibit linear $I-V$ curves (right), demonstrating ohmic conductivity with low resistance of $R = 86\ \Omega$. Such an ohmic response is indicative of continuous, metallic connections across the sample. Reprinted with permission from ref 85. Copyright 2003 National Academy of Sciences.

Besides leveraging their structural specificity to create nanoparticles array and nanowires, proteins with dynamic motility functions can add another avenue as biotemplates with applications in nanoelectromechanical systems (NEMS), e.g., as microconveyor belts for the sorting and delivery of nanomaterials. Motor proteins are cellular nanoscale machines that convert chemical energy in the form of high-energy phosphates (adenosine triphosphate, ATP) into mechanical work, e.g., intracellular transport of organelles and cell motility.[91] Kinesin is one type of cargo transporting protein motor. It uses the energy from ATP hydrolysis to step along microtubule (MT) filaments. Two practical approaches have been used to reconstitute motor proteins based on kinesin and MTs: either the kinesins move along MTs that have been fixed to a synthetic (e.g., glass) surface (motor function), or the MTs are propelled over surface-attached kinesin proteins (conveyor belt function). The first approach is advantageous for transporting larger, kinesin-functionalized materials such as beads[92] and QDs. Muthukrishnan et al. functionalized CdSe/ZnS QDs with kinesin motors via a biotin−neutravidin linkage.[93] The authors then showed that it was possible to guide the transport of kinesin−neutravidin−QD complexes by the surface-immobilized MT (Figure 8).

In the second approach, CdSe QDs were coupled to MT using a biotin−streptavidin linkage.[94] In this case, QD assembly was confined to the central region within the MTs in order to allow the MT filament ends to interact with immobilized kinesins. In this way, the kinesin motor proteins were able to successfully transport the QD−MT composites. To realize the full potential of utilizing molecular motors as

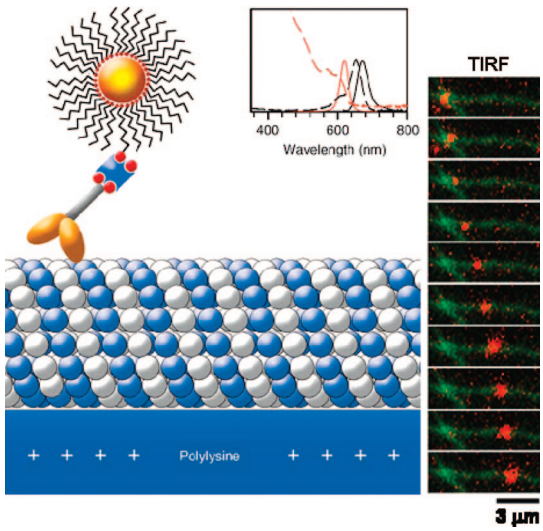

Figure 8. (Left) Schematic of a kinesin−neutravidin−QD complex moving along a surface-immobilized microtubule. (Right) TIRF image showing a QD−kinesin complex moving along an immobilized fluorescently labeled MT (elapsed time = 20 s). Reprinted with permission from ref 93. Copyright 2006 Wiley.

conveyor belts in future nanoscale devices, we must achieve fine control over transport directionality. A combination of chemical and topographical patterns can be employed to selectively bind kinesin motors and subsequently guide the motility of MTs on the kinesin-modified surfaces.[92,95]

Another example of protein motor systems is actin−myosin-based nanotransporters. The actin−myosin protein couple plays a key function in muscle mechanics. In muscle, actin forms microfilaments, which, together with myosin that forms myofibrils, provide the mechanism of contraction. As stated before, it has been clearly demonstrated that protein fibrils can serve as scaffolds for the biotemplating of metallic nanowire structures. Willner et al. has proposed the design of gold nanowires based on the use of actin filaments as metallic nanotransporters on a myosin-modified surface.[96] The design of actin−Au nanoblock patterned nanotransporters is envisioned to transport and release materials adsorbed to the gold elements at localized targets.[97–103]

5.2.2. Two-Dimensional Protein Crystals. As biological components, 2D multimeric protein complexes found in nature are nanostructures that display a truly remarkable ability to undergo molecular self-assembly with high levels of organization, complexity, and precision. The synthesis of a variety of inorganic nanostructures and arrays with a wide spectrum of morphologies by exploiting the 2D crystalline arrangements of proteins for biomolecular templating has been demonstrated in a number of reports.

5.2.2.1. Bacterial Surface Layer (S-layer) Proteins. As described in many reviews,[98–103] S-layers are 2D crystalline arrangements of proteins or glycoproteins that constitute the outermost structural component of many bacteria. S-layers are composed of identical protein subunits ranging in mass from 40 to 200 kDa. These proteins feature a highly repetitive surface structure with nanometric unit cell dimensions (i.e., 3–30 nm center-to-center spacings) and display a variety of different lattice symmetries, including oblique (p1, p2), square (p4), or hexagonal (p3, p6) arrays[99,104] with identical pore dimensions in the range of 2–8 nm diameter. The physical and chemical properties that lead to these highly repetitive structures make S-layer lattices particularly suitable for the biotemplating of molecules and nanoparticles onto these surfaces. In the field of nanotechnology, recent studies have demonstrated that the stable periodic structure of S-layers can be exploited as a robust template for forming nanostructured arrays via a number of chemical and physical approaches, including metal vapor deposition/argon ion milling,[105] wet-chemical deposition followed by electron beam irradiation,[106] and site-specific assembly of presynthesized particles.[107]

In one synthetic approach for generating ordered nanoparticle arrays on S-layers, a combination of wet and vapor-phase chemical deposition processes was employed for the in situ nucleation of the inorganic material. In a pioneering study by Shenton et al.[108] (1997), for example, it was demonstrated that native *Bacillus stearothermophilus* and *Bacillus sphaericus* could be used to induce the mineralization of CdS superlattices. In these experiments, self-assembled S-layers were exposed to a $CdCl_2$ metal−salt solution for several hours followed by slow vapor-phase reaction with a reducing agent (H_2S) over a period of one to two days. The resulting CdS nanocrystals (about 4–5 nm in size) were localized mainly to the pore regions between the subunits of the S-layers and arranged in a periodic pattern that corresponded to the oblique and square lattice symmetries of the respective S-layers.

An alternative strategy for the in situ nucleation of metal nanoparticles on a chemically modified S-layer was subsequently demonstrated by Dieluweit et al.[109] They showed that introduction of thiol groups into the primary structure of the S-layer *B. sphaericus* significantly enhanced the immobilization of gold nanoparticles on the protein template. Square arrays of Au particles with a 12.8 nm repeat distance could be fabricated upon exposure to a tetrachloroauric(III) acid solution. The isolated gold nanoparticles (4–5 nm in size) were formed in the pore regions, and the shape of the particles resembled the morphology of the pore structure itself.

A different approach involved the metallization of the native S-layer of *Sporosarcina ureae* (p4, square, 13.2 nm lattice constant) for the production of Pt nanoparticles.[110] This procedure resulted in the formation of well-separated, roughly spherical Pt^0 particles (~1.9 nm diameter) of uniform diameter distribution that were spatially aligned along the tetragonal crystalline structure of the S-layer protein template. The results from high-resolution TEM studies indicated that the Pt^0 clusters were mostly present in a purely metallic, crystalline phase with well-resolved lattice fringes.

An alternative option for the fabrication of well-ordered arrays of nanoparticles is the use of presynthesized colloids. Hall and co-workers[107] were able to show that the repetitive surface features of the S-layer from the positive bacterium *Deinococcus radiodurans* could be used to direct the periodic assembly of negatively charged gold nanoparticles (diameter = 5 nm).[107] The *D. radiodurans* S-layer, also known as the hexagonally packed intermediate (HPI) layer, comprises a hexameric protein core unit with a central pore surrounded by six relatively large openings ("vertex point"). Although

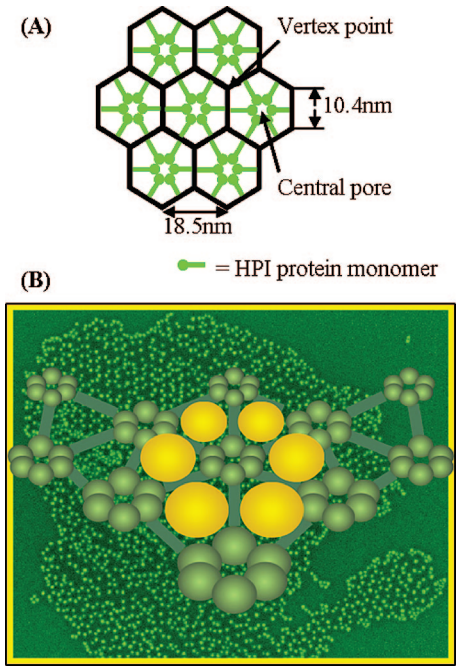

Figure 9. (A) Schematic illustration of the structure and hexagonal symmetry of the HPI S-layers. Black lines illustrate a regular hexagonal lattice model overlaid on top of the HPI layer. (B) SEM image (background) of a honeycomb-like pattern of Au nanoparticles (NPs) adsorbed on S-layer upon addition of 25 mM NaCl. Adsorption of NPs takes place at the vertex point of the S-layer as shown in the cartoon representation.

some aggregation of the deposited particles was visible, the measured interparticle center-to-center spacing (18 nm) was generally consistent with the lattice constant of the underlying S-layer template. In light of structural evidence from previous cryo-TEM studies,[111] which showed that each hexameric protein unit is approximately conical in shape and contains a central pore region ~2 nm wide, the authors suggested that the Au nanoparticles were most likely bound to the HPI layer central pore through electrostatic binding. However, Bergkvist et al. subsequently showed that the nanoparticle binding in fact takes place at the vertex regions of the HPI layer, and because of the presence of interparticle repulsion forces of the negatively charged citrate-stabilized Au colloids, adsorption tends to be at every second vertex point.[31]

Further studies of gold nanoparticle binding to the HPI S-layer by Bergkvist et al. revealed that upon increasing the ionic strength of the nanoparticle solution, ordered packing was still observed. However, because interparticle repulsions were less prominent under these conditions, adsorption of nanoparticles occurred in virtually every available vertex point, resulting in the formation of a honeycomb-like pattern of nanoparticles extending throughout the HPI monolayer sheet (Figure 9).

In later work by the same group, Mark et al. demonstrated the ability of two different types of S-layer proteins (isolated from *D. radiodurans* (HPI) and the thermoacidophilic archaeon *Sulfolobus acidocaldarius* (SAS)) displaying distinctive lattice spacing and geometrical arrangements to form self-organized, ordered arrays of metallic and semiconducting nanoparticles.[112] Various species of CdSe/ZnS core−shell QDs functionalized with different types of thiol ligands (negative or positive charged/short- or long-chain length) as

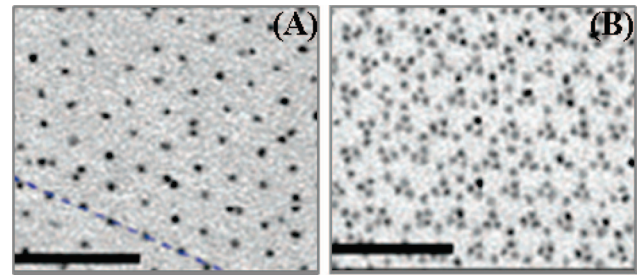

Figure 10. Bright-field TEM images of different nanoparticles patterns on unstained SAS S-layers after incubation in solutions of QDs functionalized with 7-carboxy-1-heptanethiol ligands. Figures A and B are hypothesized to correspond to particle adsorption to the two different "faces" of the SAS S-layer. Scale bars = 100 nm. Reprinted with permission from ref 32. Copyright 2006 American Chemical Society.

well as dendrimer-encapsulated platinum nanoparticles (Pt-DENs)[113] were successfully templated. Importantly, it was further shown that by choosing appropriate NP surface ligands, it was possible to tailor, within certain limits, the particle size−surface interactions to complement the topochemistry of the protein lattice substrate. In a striking case, the biotemplating of 7-carboxy-1-heptanethiol ligand-capped QDs on the SAS S-layers led to small polygonal clusters comprising three QDs arranged with 3-fold rotational symmetry around isolated QDs (Figure 10).

These results suggest that the SAS-layer can biologically program the formation of uniform arrays of spatially complex arrangements of NP clusters without requiring any specific interparticle bridging molecules.

A fusion of bottom-up self-assembly and top-down lithographic approaches may provide another possible means to better control the placement of materials as well as provide a wider range of potential nanostructure morphologies. For example, the use of S-layers as templates for thin-film lithographic processing to create ordered metallic nanostructures was originally described in a series of reports by Douglas and co-workers.[114–116] In one early approach,[114] S-layer patches isolated from *S. acidocaldarius* (SAS) were attached to a freshly cleaved highly oriented pyrolytic graphite substrate and shadowed at an angle with titanium (Ti) to produce a mask for the subsequent formation of a periodic array of nanometric holes (~10 nm in diameter) by ion milling (Figure 11).

In a further extension of the protein masking/etching technique to more technologically relevant substrates, Winningham et al.[116] achieved pattern transfer from an S-layer biomolecular nanomask ("bionanomask") to crystalline silicon (Si) substrates by using an inductively coupled plasma (ICP) etch process. In this newer methodology, a so-called intermediate transfer layer (ITL) comprising a layer of a resist-like material (e.g., nitrocellulose, polyimide, etc.) is first applied to the silicon substrate before deposition of the S-layer. The bionanomask pattern is first transferred to the ITL and then to the substrate. By optimizing the ICP etch and/or metal lift-off parameters, the authors were able to use *S. acidocaldarius* S-layers deployed on an ITL of ultrathin (<10 nm) nitrocellulose to pattern Si substrates with either a 2D ordered array of ~10 nm diameter holes or, alternatively, a 2D array of ~10 nm diameter metal dots (Ti, Pd,

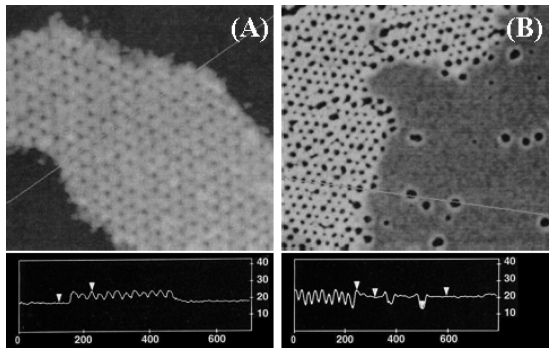

Figure 11. Transfer of S-layer-derived nanometer-scale patterns to highly oriented pyrolytic graphite (HOPG) surfaces by ion milling. (A) AFM image of TiO*x*-coated on-S-layer and off-S-layer areas before fast atom beam (FAB) milling. The S-layer lattice constant of 22 nm serves to indicate the length scale of the image. The cross-section profile along the line in the AFM image is also shown. (B) AFM image of TiO*x*-coated on-S-layer and off-S-layer areas after FAB milling. Reprinted with permission from ref 114. Copyright 1992 American Association for the Advancement of Science.

or Au). Both types of arrays displayed hexagonal symmetry and a lattice constant of 22 nm, in agreement with the morphological structure of the protein bionanomask with the exception of occasional defects.

The possibility of using S-layer/nanoparticle templates for the bionanofabrication of silicon nanopillar structures has been recently explored. Mark et al. successfully employed an inductively coupled plasma (ICP) SiC_4 etch process to create 100 nm high silicon nanopillars using an etch mask generated from 5 nm Au nanoparticles adsorbed onto the HPI S-layer.[117] On the other hand, the resulting silicon nanopillar structures (8–13 nm wide at the tip, 15–20 nm wide at half-height, 20–30 nm wide at the base, and 60–90 nm tall) appeared to lack any significant degree of translational ordering. These results suggest that further studies are needed in order to elucidate the optimal plasma processing parameters that will lead to the generation of long-range ordered arrays of silicon-based nanostructures using S-layer protein templates.

Finally, the sensing potential of S-layer protein membranes has also been investigated,[118] although not extensively. S-layer membranes were adsorbed on an electrically conductive silicon surface and the gating characteristics of the device toward various ionic species were evaluated using electrochemical impedance spectroscopy (EIS). The system showed enhanced sensitivity toward cations, especially calcium (Ca^{2+}) ions, whose presence caused a strong ionic current, attributed to selective calcium transport through the pores of the protein membrane. This work provided evidence that S-layer pores can act as ion selective nanopore systems, with performance characteristics comparable to synthetic nanopores.[119]

5.2.2.2. Ferritin. In some cases, the protein components that have been employed for biotemplating experiments do not naturally form planar arrays in vivo. Ferritin is an intracellular iron storage protein found in both prokaryotic and eukaryotic organisms. Okuda et al. demonstrated that by inducing the artificial crystallization of ferritin molecules in vitro at a water–air interface, hexagonally close-packed 2D arrays of iron nanoparticles (diameter = 5.8 ± 1.0 nm) and indium nanoparticles (diameter = 6.6 ± 0.5 nm) could be successfully produced.[120] The self-assembled Fe−ferritin and In−ferritin nanoparticle arrays showed a high degree of uniformity, and arrays of more than 1 μm^2 in area were obtained by transferring the crystal films onto a silicon wafer. One drawback of the approach, however, is that formation of the particle arrays required the use of an aqueous subphase, where a number of critical factors that affected the spreading of the ferritin protein solutions at the surface (e.g., subphase density, surface tension, divalent ion concentration, etc.) all had to be carefully controlled.

5.2.2.3. Heat Shock Proteins. The intracellular heat-shock protein TF55β from *Sulfolobus shibatae* spontaneously assembles into an octadecameric double-ring cage structure, called a chaperonin, with nine subunits per ring and a 10 nm diameter core. Trent and colleagues used *S. shibatae* to direct the chemical synthesis of hexagonally packed metallic arrays.[121] To render the topochemical properties of TF55β suitable for in situ nanoparticle synthesis, the authors genetically removed a loop that occludes the central pore of the assembled chaperonin and fused a polyhistidine (His_{10}) sequence to its amino terminus. With these modifications, the solvent-accessible cores of assembled chaperonins displayed 180 additional His residues, creating a region with enhanced affinity for metal ions that was spatially constrained by the interior dimensions of the chaperonin. When incubated with Pd^{2+}, the chaperonin cores acted as sites for selectively initiating the chemical reduction of magnetic transition metal (TM) ions (either Ni^{2+} or Co^{2+}) from precursor salts. This procedure yielded bimetallic metal (Ni−Pd or Co−Pd) arrays with lattice dimensions defined by the engineered chaperonin.

As shown by the many examples described above, significant developments have been made in the area of protein-based biotemplating of nanostructured materials during the last several years. Clearly, proteins as well as other types of biological macromolecules will continue to assume increasingly prevalent roles in the future development of new functional materials through nanobiotechnology. Such advanced materials are expected to find diverse applications in a number of areas ranging from optoelectronics to catalysis.

6. Concluding Remarks

6.1. Advantages and Limitations of the Biotemplating Approach. This short review highlighted some of the most recent advances that have been developed in the biotemplating of nanostructured materials. Notable advantages of biotemplating in nanostructure fabrication include the sheer structural diversity of available biological species and materials, as well as the sophisticated architectures (1D, 2D, and 3D) and degree of complexity achievable. Together, these elements provide for the creation of a diverse range of novel materials with an unprecedented repertoire of dimensions (resolution <100 nm) and morphologies that extend beyond what is currently possible with conventional lithography/etching techniques. The biotemplating approach is also potentially more cost- and time-effective (parallel fabrication approach) when compared with current serial techniques (e.g., electron beam lithography, X-ray lithography) for nanostructure fabrication. In addition, the repetitive to-

pochemical features and variety of functional groups found in many biological materials, can be exploited for the in situ synthesis and directed self-assembly of both organic and inorganic nanostructures under mild conditions without the use of harsh chemical treatments. And finally, biotemplates are also highly amenable to very (spatially) precise modifications at the molecular level through rational genetic engineering and/or targeted chemical modifications. Taken together, these attributes lead to a "biomolecular tool-kit" that offers great diversity and a facile approach for the fabrication of a variety of structures and devices. The full range of possibilities that biological templates have to offer has only just started to be explored. Indeed, researchers are just beginning to grasp an understanding of the effects of nanoscale topographies on the optical, chemical, and electrical properties of materials. On the basis of these initial reports, there is clearly great potential for using biological materials to develop entirely new types of sensing systems that display superior selectivity and sensitivity over existing conventional designs.

However, for biotemplating to become more established as a reliable nanofabrication approach, several limitations that currently exist will need to be overcome. Most notably, as the biotemplating technique is a relatively new approach, it still lacks the high yield levels and precise uniformity provided by other synthetic fabrication methods. In particular, large-scale fabrication may be an issue in some cases because of a lack of sufficient quantities of purified biological material, or because of a lack of long-range order in the final product due to intrinsic lattice/morphological defects in the biotemplate itself. Moreover, because the exact mechanisms by which biological entities form defined patterns and direct the growth of crystalline materials are not yet fully understood, biotemplating studies are often conducted in a highly empirical manner. This often requires a significant amount of effort to be spent in trial and error experiments, with results that are in some cases neither predictable nor always repeatable. Finally, there remains a great need for scientists to develop a better understanding of the biological−materials interface in general. Current surface functionalization methods for the creation of engineered substrates for the deterministic, oriented attachment of biological molecules still lack the degree of control necessary to be useable on a large scale, such that high quality and high uniformity can be reproducibly achieved.

6.2. Perspectives and Future Directions. As our understanding of the natural world improves, so does our ability to harness the power of biological systems and put it to work to drive technological innovation. Without a doubt, transfer of knowledge through interdisciplinary collaborations among scientists from several diverse fields of study, such as molecular self-assembly, engineering, and biophysics, will continue to facilitate the advancement of biotemplating at a rapid pace. Ultimately, it is expected that the biotemplating approach will provide innovative means to construct novel molecular architectures with greater speed (parallel fabrication), precision, and flexibility, and at a lower cost when compared to traditional manufacturing processes.

Acknowledgment. This work was supported by the National Science Foundation under a Nanoscale Interdisciplinary Research Team (NIRT) Grant (NSF-0403990).

References

(1) Cui, Y. B.; M, T.; Liddle, J. A.; Sonnichsen, C.; Boussert, B.; Alivisatos, A. P. *Nano Lett.* **2004**, *4*, 1093–1098.
(2) Ohshima, T.; Song, H. Z.; Okada, Y.; Akahane, K.; Miyazawa, T.; Kawabe, M.; Yokoyama, N. *Phys. Status Solidi C* **2003**, *0* (4), 1364–1367.
(3) Fischbein, M. D.; Drndic, M. *Appl. Phys. Lett.* **2005**, *86*, 193106.
(4) Yonzon, C. R.; Stuart, D. A.; Zhang, X.; McFarland, A. D.; Haynes, C. L.; Van Duyne, R. P. *Talanta* **2005**, *67*, 438–448.
(5) Grunes, J.; Zhu, J.; Anderson, E. A.; Somorjai, G. A. *J. Phys. Chem. B* **2002**, *106*, 11463–11468.
(6) Rybczynski, J.; Banerjee, D.; Kosiorek, A.; Giersig, M.; Ren, Z. F. *Nano Lett.* **2004**, *4* (10), 2037–2040.
(7) Lei, Y.; Yeong, K.-S.; Thong, J. T. L.; Chim, W.-K. *Chem. Mater.* **2004**, *16* (14), 2757–2761.
(8) Cao, Y. C.; Jin, R.; Mirkin, C. A. *Science* **2002**, *297* (5586), 1536–1540.
(9) Zheng, G.; Patolsky, F.; Cui, Y.; Wang, W. U.; Lieber, C. M. *Nat. Biotechnol.* **2005**, *23* (10), 1294–1301.
(10) Wan, Q.; Feng, P.; Wang, T. H. *Appl. Phys. Lett.* **2006**, *89* (12), 123102/1–123102/3.
(11) Wu, M.; Yao, L.; Cai, W.; Jiang, G.; Li, X.; Yao, Z. *J. Mater. Sci. Technol.* **2004**, *20* (1), 11–13.
(12) Tseng, A. A.; Notargiacomo, A.; Chen, T. P. *J. Vac. Sci. Technol., B* **2005**, *23* (3), 877–894.
(13) Huck, W. T. S. *Angew. Chem., Int. Ed.* **2007**, *46* (16), 2754–2757.
(14) Li, X.-M.; Huskens, J.; Reinhoudt, D. N. *J. Mater. Chem.* **2004**, *14* (20), 2954–2971.
(15) Gates, B. D.; Xu, Q.; Stewart, M.; Ryan, D.; Willson, C. G.; Whitesides, G. M. *Chem. Rev.* **2005**, *105* (4), 1171–1196.
(16) Madou, M. J. *Fundamentals of Microfabrication: The Science of Miniaturization*, 2nd ed.; CRC Press: Boca Raton, FL, 2002.
(17) Salaita, K.; Wang, Y.; Fragala, J.; Vega, R. A.; Liu, C.; Mirkin, C. A. *Angew. Chem., Int. Ed.* **2006**, *45* (43), 7220–7223.
(18) Lazzari, M.; Lopez-Quintela, M. A. *Adv. Mater.* **2003**, *15* (19), 1583–1594.
(19) Park, C.; Yoon, J.; Thomas, E. L. *Polymer* **2003**, *44*, 6725–6760.
(20) Klefenz, H. *Eng. Life Sci.* **2004**, *4*, 211–218.
(21) Gazit, E. *FEBS J.* **2007**, *274* (2), 317–322.
(22) Sanchez, C.; Arribart, H.; Madeleine, M.; Guille, G. *Nat. Mater.* **2005**, *4* (4), 277–288.
(23) Huang, J.; Wang, X.; Wang, Z. L. *Nano Lett.* **2006**, *6* (10), 2325–2331.
(24) Payne, E. K.; Rosi, N. L.; Xue, C.; Mirkin, C. A. *Angew. Chem., Int. Ed.* **2005**, *44* (32), 5064–5067.
(25) Mogul, R.; Getz Kelly, J. J.; Cable, M. L.; Hebard, A. F. *Mater. Lett.* **2005**, *60* (1), 19–22.
(26) Blum, A. S.; Soto, C. M.; Wilson, C. D.; Cole, J. D.; Kim, M.; Gnade, B.; Chatterji, A.; Ochoa, W. F.; Lin, T.; Johnson, J. E.; Ratna, B. R. *Nano Lett.* **2004**, *4* (5), 867–870.
(27) Knez, M.; Bittner, A. M.; Boes, F.; Wege, C.; Jeske, H.; Mai, E.; Kern, K. *Nano Lett.* **2003**, *3* (8), 1079–1082.
(28) Mao, C.; Solis, D. J.; Reiss, B. D.; Kottmann, S. T.; Sweeney, R. Y.; Hayhurst, A.; Georgiou, G.; Iverson, B.; Belcher, A. M. *Science* **2004**, *303* (5655), 213–217.
(29) Behrens, S.; Rahn, K.; Habicht, W.; Bohm, K. J.; Rosner, H.; Dinjus, E.; Unger, E. *Adv. Mater.* **2002**, *14* (22), 1621–1625.
(30) Behrens, S.; Habicht, W.; Wagner, K.; Unger, E. *Adv. Mater.* **2006**, *18*, 284-+.
(31) Bergkvist, M.; Mark, S. S.; Yang, X.; Angert, E. R.; Batt, C. A. *J. Phys. Chem. B* **2004**, *108* (24), 8241–8248.
(32) Mark, S. S.; Bergkvist, M.; Yang, X.; Teixeira, L. M.; Bhatnagar, P.; Angert, E. R.; Batt, C. A. *Langmuir* **2006**, *22* (8), 3763–3774.
(33) Park, S. H.; Yan, H.; Reif, J. H.; LaBean, T. H.; Finkelstein, G. *Nanotechnology* **2004**, *15* (10), S525–S527.
(34) Caruso, R. A. *Angew. Chem., Int. Ed.* **2004**, *43* (21), 2746–2748.
(35) Seeman, N. C.; Belcher, A. M. *Proc. Natl. Acad. Sci. U.S.A.* **2002**, *99* (9, Suppl. 2), 6451–6455.
(36) Zhang, W.; Zhang, D.; Fan, T.; Ding, J.; Guo, Q.; Ogawa, H. *Nanotechnology* **2006**, *17* (3), 840–844.
(37) Potyrailo, R. A.; Ghiradella, H.; Vertiatchikh, A.; Dovidenko, K.; Cournoyer, J. R.; Olson, E. *Nat. Photonics* **2007**, *1* (2), 123–128.
(38) Sumper, M.; Brunner, E. *Adv. Funct. Mater.* **2006**, *16* (1), 17–26.
(39) Rosi, N. L.; Thaxton, C. S.; Mirkin, C. A. *Angew. Chem., Int. Ed.* **2004**, *43* (41), 5500–5503.
(40) Losic, D.; Mitchell, J. G.; Voelcker, N. H. *New J. Chem.* **2006**, *30* (6), 908–914.
(41) De Stefano, L.; Rendina, I.; De Stefano, M.; Bismuto, A.; Maddalena, P. *Appl. Phys. Lett.* **2005**, *87* (23), 233902/1–233902/3.
(42) Zhou, H.; Fan, T.; Zhang, D.; Guo, Q.; Ogawa, H. *Chem. Mater.* **2007**, *19* (9), 2144–2146.
(43) Zhang, B.; Davis, S. A.; Mann, S.; Mendelson, N. H. *Chem. Commun.* **2000**, (9), 781–782.
(44) Berry, V.; Rangaswamy, S.; Saraf, R. F. *Nano Lett.* **2004**, *4* (5), 939–942.

(45) Douglas, T.; Young, M. *Nature* **1998**, *393* (6681), 152–155.
(46) Shenton, W.; Douglas, T.; Young, M.; Stubbs, G.; Mann, S. *Adv. Mater.* **1999**, *11* (3), 253–256.
(47) Dujardin, E.; Peet, C.; Stubbs, G.; Culver, J. N.; Mann, S. *Nano Lett.* **2003**, *3* (3), 413–417.
(48) Fowler, C. E.; Shenton, W.; Stubbs, G.; Mann, S. *Adv. Mater.* **2001**, *13* (16), 1266–1269.
(49) Tsukamoto, R.; Muraoka, M.; Seki, M.; Tabata, H.; Yamashita, I. *Chem. Mater.* **2007**, *19* (10), 2389–2391.
(50) Radloff, C.; Vaia, R. A.; Brunton, J.; Bouwer, G. T.; Ward, V. K. *Nano Lett.* **2005**, *5* (6), 1187–1191.
(51) Zhang, Z.; Buitenhuis, J. *Small* **2007**, *3* (3), 424–428.
(52) Mao, C.; Flynn, C. E.; Hayhurst, A.; Sweeney, R.; Qi, J.; Georgiou, G.; Iverson, B.; Belcher, A. M. *Proc. Natl. Acad. Sci. U.S.A.* **2003**, *100* (12), 6946–6951.
(53) Huang, Y.; Chiang, C.-Y.; Lee, S. K.; Gao, Y.; Hu, E. L.; De Yoreo, J.; Belcher, A. M. *Nano Lett.* **2005**, *5* (7), 1429–1434.
(54) Ogasawara, T.; Debart, A.; Holzapfel, M.; Novak, P.; Bruce, P. G. *J. Am. Chem. Soc.* **2006**, *128* (4), 1390–1393.
(55) Kunduraci, M.; Al-Sharab, J. F.; Amatucci, G. G. *Chem. Mater.* **2006**, *18* (15), 3585–3592.
(56) Nam, K. T.; Kim, D.-W.; Yoo, P. J.; Chiang, C.-Y.; Meethong, N.; Hammond, P. T.; Chiang, Y.-M.; Belcher, A. M. *Science* **2006**, *312* (5775), 885–888.
(57) Zhang, S. *Nat. Biotechnol.* **2003**, *21* (10), 1171–1178.
(58) Payne, G. F. *Curr. Opin. Chem. Biol.* **2007**, *11* (2), 214–219.
(59) Gazit, E. *Chem. Soc. Rev.* **2007**, *36* (8), 1263–1269.
(60) Reches, M.; Gazit, E. *Science* **2003**, *300* (5619), 625–627.
(61) Djalali, R.; Chen, Y.-f.; Matsui, H. *J. Am. Chem. Soc.* **2002**, *124* (46), 13660–13661.
(62) Browning, S. L.; Lodge, J.; Price, R. R.; Schelleng, J.; Schoen, P. E.; Zabetakis, D. *J. Appl. Phys.* **1998**, *84* (11), 6109–6113.
(63) Lvov, Y. M.; Price, R. R.; Selinger, J. V.; Singh, A.; Spector, M. S.; Schnur, J. M. *Langmuir* **2000**, *16* (14), 5932–5935.
(64) Seeman, N. C. *Nature* **2003**, *421* (6921, Suppl.), 427–431.
(65) Niemeyer, C. M. *Curr. Opin. Chem. Biol.* **2000**, *4* (6), 609–618.
(66) Tanaka, K.; Shionoya, M. *Chem. Lett.* **2006**, *35* (7), 694–699.
(67) Gu, Q.; Cheng, C.; Gonela, R.; Suryanarayanan, S.; Anabathula, S.; Dai, K.; Haynie, D. T. *Nanotechnology* **2006**, *17* (1), R14–R25.
(68) Lin, C.; Liu, Y.; Rinker, S.; Yan, H. *ChemPhysChem* **2006**, *7* (8), 1641–1647.
(69) Stanca, S. E.; Ongaro, A.; Eritja, R.; Fitzmaurice, D. *Nanotechnology* **2005**, *16* (9), 1905–1911.
(70) Sharma, J.; Chhabra, R.; Liu, Y.; Ke, Y.; Yan, H. *Angew. Chem., Int. Ed.* **2006**, *45* (5), 730–735.
(71) Dong, L.; Hollis, T.; Connolly, B. A.; Wright, N. G.; Horrocks, B. R.; Houlton, A. *Adv. Mater.* **2007**, *19* (13), 1748–1751.
(72) Kumar, A.; Pattarkine, M.; Bhadbhade, M.; Mandale, A. B.; Ganesh, K. N.; Datar, S. S.; Dharmadhikari, C. V.; Sastry, M. *Adv. Mater.* **2001**, *13* (5), 341–344.
(73) Kinsella, J. M.; Ivanisevic, A. *Langmuir* **2007**, *23* (7), 3886–3890.
(74) Shemer, G.; Krichevski, O.; Markovich, G.; Molotsky, T.; Lubovitz, I.; Kotlyar, A. B. *J. Am. Chem. Soc.* **2006**, *128* (34), 11006–11007.
(75) Patolsky, F.; Weizmann, Y.; Lioubashevski, O.; Willner, I. *Angew. Chem., Int. Ed.* **2002**, *41* (13), 2323–2327.
(76) Stsiapura, V.; Sukhanova, A.; Baranov, A.; Artemyev, M.; Kulakovich, O.; Oleinikov, V.; Pluot, M.; Cohen, J. H. M.; Nabiev, I. *Nanotechnology* **2006**, *17* (2), 581–587.
(77) Feldkamp, U.; Niemeyer, C. M. *Angew. Chem., Int. Ed.* **2006**, *45* (12), 1856–1876.
(78) Zhang, J.; Liu, Y.; Ke, Y.; Yan, H. *Nano Lett.* **2006**, *6* (2), 248–251.
(79) Wang, Y.; Lu, L.; Zheng, Y.; Chen, X. *J. Biomed. Mater. Res., Part A* **2006**, *76A*, 589–595.
(80) Aldaye, F. A.; Sleiman, H. F. *J. Am. Chem. Soc.* **2007**, *129* (14), 4130–4131.
(81) Scheibel, T. *Curr. Opin. Biotechnol.* **2005**, *16* (4), 427–433.
(82) Kumara, M. T.; Tripp, B. C.; Muralidharan, S. *J. Phys. Chem. C* **2007**, *111* (14), 5276–5280.
(83) Behrens, S.; Wu, J.; Habicht, W.; Unger, E. *Chem. Mater.* **2004**, *16* (16), 3085–3090.
(84) Behrens, S.; Habicht, W.; Wu, J.; Unger, E. *Surf. Interface Anal.* **2006**, *38* (6), 1014–1018.
(85) Scheibel, T.; Parthasarathy, R.; Sawicki, G.; Lin, X.-M.; Jaeger, H.; Lindquist, S. L. *Proc. Natl. Acad. Sci. U.S.A.* **2003**, *100* (8), 4527–4532.
(86) Hamada, D.; Yanagihara, I.; Tsumoto, K. *Trends Biotechnol.* **2004**, *22* (2), 93–97.
(87) Habicht, W.; Behrens, S.; Unger, E.; Dinjus, E. *Surf. Interface Anal.* **2006**, *38* (4), 194–197.
(88) Ferguson, N.; Becker, J.; Tidow, H.; Tremmel, S.; Sharpe, T. D.; Krause, G.; Flinders, J.; Petrovich, M.; Berriman, J.; Oschkinat, H.; Fersht, A. R. *Proc. Natl. Acad. Sci. U.S.A.* **2006**, *103* (44), 16248–16253.
(89) Kumara, M. T.; Tripp, B. C.; Muralidharan, S. *Chem. Mater.* **2007**, *19* (8), 2056–2064.
(90) Kumara, M. T.; Srividya, N.; Muralidharan, S.; Tripp, B. C. *Nano Lett.* **2006**, *6* (9), 2121–2129.
(91) Mansson, A.; Sundberg, M.; Bunk, R.; Balaz, M.; Nicholls, I. A.; Omling, P.; Tegenfeldt, J. O.; Tagerud, S.; Montelius, L. *IEEE Trans. Adv. Packag.* **2005**, *28* (4), 547–555.
(92) Hess, H.; Clemmens, J.; Qin, D.; Howard, J.; Vogel, V. *Nano Lett.* **2001**, *1* (5), 235–239.
(93) Muthukrishnan, G.; Hutchins, B. M.; Williams, M. E.; Hancock, W. O. *Small* **2006**, *2* (5), 626–630.
(94) Bachand, G. D.; Rivera, S. B.; Boal, A. K.; Gaudioso, J.; Liu, J.; Bunker, B. C. *Nano Lett.* **2004**, *4* (5), 817–821.
(95) van den Heuvel, M. G. L.; Butcher, C. T.; Smeets, R. M. M.; Diez, S.; Dekker, C. *Nano Letters* **2005**, *5* (6), 1117–1122.
(96) Patolsky, F.; Weizmann, Y.; Willner, I. *Nat. Mater.* **2004**, *3* (10), 692–695.
(97) Mertig, M.; Kirsch, R.; Pompe, W. *Appl. Phys. A: Mater. Sci. Process.* **1998**, *66*, S723–S727.
(98) Pum, D.; Schuster, B.; Sara, M.; Sleytr, U. B. *IEEE Proc. Nanobiotechnology* **2004**, *151* (3), 83–6.
(99) Sára, M.; Pum, D.; Schuster, B.; Sleytr, U. B. *J. Nanosci. Nanotechnol.* **2005**, *5*, 1939–1953.
(100) Sleytr, U. B.; Gyorvary, E.; Pum, D. *Prog. Org. Coat.* **2003**, *47* (3–4), 279–287.
(101) Sleytr, U. B.; Messner, P.; Pum, D.; Sára, M. *Angew. Chem., Int. Ed.* **1999**, *38*, 1034–1054.
(102) Sleytr, U. B.; Sára, M.; Pum, D.; Schuster, B., Crystalline bacterial cell surface layers (S-layers): A versatile self-assembly system. In *Supramolecular Polymers*, 2nd ed.; Ciferri, A., Ed.; CRC Press: Boca Raton, FL, 2005; pp 583–616.
(103) Sleytr, U. B.; Sara, M.; Pum, D.; Schuster, B.; Messner, P.; Schaffer, C. Self-assembly protein systems: Microbial S-layers. In *Biopolymers*, Steinbuechel, A., Ed.Wiley-VCH Verlag GmbH: Weinheim, 2003; *Vol. 7*, pp285–338.
(104) Bossmann, S. H. S-layer proteins in bioelectronic applications. In *Bioelectronics: From Theory to Applications*; Willner, I., Katz, E., Eds.; Wiley-VCH Verlag GmbH & Co. KGaA: Weinheim, Germany, 2005; pp 395–426.
(105) Panhorst, M.; Brückl, H.; Kiefer, B.; Reiss, G.; Santarius, U.; Guckenberger, R. *J. Vac. Sci. Technol., B* **2001**, *19* (3), 722–724.
(106) Wahl, R.; Mertig, M.; Raff, J.; Selenska-Pobell, S.; Pompe, W. *Adv. Mater.* **2001**, *13* (10), 736–740.
(107) Hall, S. R.; Shenton, W.; Engelhardt, H.; Mann, S. *ChemPhysChem* **2001**, *2* (3), 184–186.
(108) Shenton, W.; Pum, D.; Sleytr, U. B.; Mann, S. *Nature* **1997**, *389* (6651), 585–587.
(109) Dieluweit, S.; Pum, D.; Sleytr, U. B. *Supramol. Sci.* **1998**, *5* (1–2), 15–19.
(110) Mertig, M.; Wahl, R.; Lehmann, M.; Simon, P.; Pompe, W. *Eur. Phys. J. D* **2001**, *16* (1–3), 317–320.
(111) Baumeister, W.; Barth, M.; Hegerl, R.; Guckenberger, R.; Hahn, M.; Saxton, W. O. *J. Mol. Biol.* **1986**, *187* (2), 241–250.
(112) Reference removed at galley stage.
(113) Mark, S. S.; Bergkvist, M.; Yang, X.; Angert, E. R.; Batt, C. A. *Biomacromolecules* **2006**, *7* (6), 1884–1897.
(114) Douglas, K.; Devaud, G.; Clark, N. A. *Science* **1992**, *257* (5070), 642–644.
(115) Winningham, T. A.; Gillis, H. P.; Chouto, D. A.; Martin, K. P.; Moore, J. T.; Douglas, K. *Surf. Sci.* **1998**, *406* (1–3), 221–228.
(116) Winningham, T. A.; Whipple, S. G.; Douglas, K. *J. Vac. Sci. Technol., B* **2001**, *19* (5), 1796–1802.
(117) Mark, S. S.; Bergkvist, M.; Bhatnagar, P.; Welch, C.; Goodyear, A. L.; Yang, X.; Angert, E. R.; Batt, C. A. *Colloids Surf., B* **2007**, *57* (2), 161–73.
(118) Sotiropoulou, S.; Mark, S. S.; Angert, E. R.; Batt, C. A. *J. Phys. Chem. C* **2007**, *111* (35), 13232–13237.
(119) Siwy, Z. S.; Powell, M. R.; Petrov, A.; Kalman, E.; Trautmann, C.; Eisenberg, R. S. *Nano Lett.* **2006**, *6* (8), 1729–1734.
(120) Okuda, M.; Kobayashi, Y.; Suzuki, K.; Sonoda, K.; Kondoh, T.; Wagawa, A.; Kondo, A.; Yoshimura, H. *Nano Lett.* **2005**, *5* (5), 991–993.
(121) McMillan, R. A. H. J.; Zaluzec, N. J.; Kagawa, H. K.; Mogul, R.; Li, Y.-F.; Paavola, C. D.; Trent, J. D. *J. Am. Chem. Soc.* **2005**, *127*, 10096–10100.
(122) Yan, H.; Park, S. H.; Finkelstein, G.; Reif, J. H.; LaBean, T. H. *Science* **2003**, *301*, 1882–1884.

CM702152A